

# Compact High-Isolation Dual-Polarized Antenna with AMC Reflector

Kaining Zhu, Ming Su<sup>\*</sup>, Cuiping Yu, and Yuanan Liu

**Abstract**—This paper presents a compact high-isolation dual-polarized dipole antenna with an artificial magnetic conductor (AMC) reflector. The proposed antenna is composed of a radiating element, two short pins and a  $7 \times 7$  AMC array. By introducing two short pins, the port isolation is lower than  $-33$  dB in the whole band on two ports. With the ring and AMC reflector, the dimension of the proposed antenna is only  $0.36\lambda_0 \times 0.36\lambda_0 \times 0.16\lambda_0$  at 2.2 GHz. The antenna also achieves a 10-dB return loss bandwidth from 1.6 to 2.78 GHz (54%) for both ports. The gain of the proposed antenna is around 8 dBi, and the cross-polarization is about 30 dB. Due to these properties, the proposed antenna can be applied to 2G/3G/long term evolution (LTE) base station and WLAN/WiMAX applications.

## 1. INTRODUCTION

With the tremendous growth of wireless communication technology, the way to increase channel capacity and resist multipath fading is in great demand. Therefore, compact base station antenna designs are facing many new strict demands and challenges.

Plenty of dual-polarized base station antennas have been developed [1–14]. Antennas presented in [1–5] all take full advantage of bow-tie antennas to achieve a planar structure and widen the impedance bandwidth. The antennas presented in [4, 5] both make use of short pins to improve the port isolation and etch slots to realize a property of wide bandwidth.

However, all those conventional dual-polarized antennas mentioned in [1–5] are about  $\lambda/4$  in height, which does not fulfill the development tendency to antenna miniaturization. Magneto-electric (ME) dipole antennas are also used to design dual-polarized antennas [6–8]. These ME dipole antennas all featured low profile, wide bandwidth, and stable radiations, but the sizes of the planar patches of the ME dipole antennas are larger than that of the traditional dual-polarized dipole antennas.

Replacing the conventional perfect electric conductor (PEC) reflector with an AMC reflector is an appropriate way to reduce the profile of dual-polarized antennas [9–14]. AMC is a novel material which is comparable with the ideal magnetic conductor during a certain frequency band [9]. The phase of the incident wave of AMC reflector is consistent with that of the reflected wave [10]. Thus, antennas can be placed very close to the AMC reflector without being influenced by the mirror current which is caused by using the PEC reflector. If the parameters of AMC reflector are designed carefully, it can be used to reduce the profile of dual-polarized antennas and improve the radiation performances of antennas [9–14]. Antennas proposed in [9, 10] both have compact structures, but the bandwidths are narrow. Although the bandwidths of antennas presented in [11–13] satisfy LTE base station and the profiles of the antennas are low, the overall sizes of the antennas are large.

In this paper, a compact high-isolation dual-polarized dipole antenna excited by two coaxial cables is presented. High port isolation about 33 dB and wide impedance bandwidth from 1.6 GHz to 2.78 GHz

---

*Received 14 July 2018, Accepted 19 August 2018, Scheduled 29 August 2018*

<sup>\*</sup> Corresponding author: Ming Su (suming@bupt.edu.cn).

The authors are with the Beijing Key Laboratory of Work Safety Intelligent Monitoring, School of Electronic Engineering, Beijing University of Posts and Telecommunications, Beijing 100876, China.

for both ports are achieved. The dimension of the proposed antenna is only  $50 \text{ mm} \times 50 \text{ mm} \times 22.5 \text{ mm}$  ( $0.36\lambda_0 \times 0.36\lambda_0 \times 0.16\lambda_0$ ). The cross-polarization of the proposed antenna is about 30 dB, and the gain of the proposed antenna is around 8 dBi with the efficiency of 76%.

The paper is organized as follows. Section 1 provides the research background introduction. Section 2 shows the details of antenna structure design. Simulated and measured results, discussions of some key design parameters are given in Section 3. A brief conclusion is presented in Section 4.

## 2. ANTENNA DESIGN

### 2.1. Antenna Geometry

The configuration of the proposed antenna is shown in Fig. 1. The proposed antenna mainly consists of a radiation element, two short pins and a  $7 \times 7$  AMC array. The presented radiating element is made up of two orthogonal bowtie dipoles and a circular ring. The substrate uses FR4 with a dielectric constant of 4.4, loss tangent of 0.02, and thickness of 0.8 mm. For the convenience of antenna feed, there are two via holes and a  $5.6 \text{ mm} \times 5.6 \text{ mm}$  square hole in the substrate. Moreover, the radiating element radiates  $0^\circ$  and  $90^\circ$  linearly polarized waves.

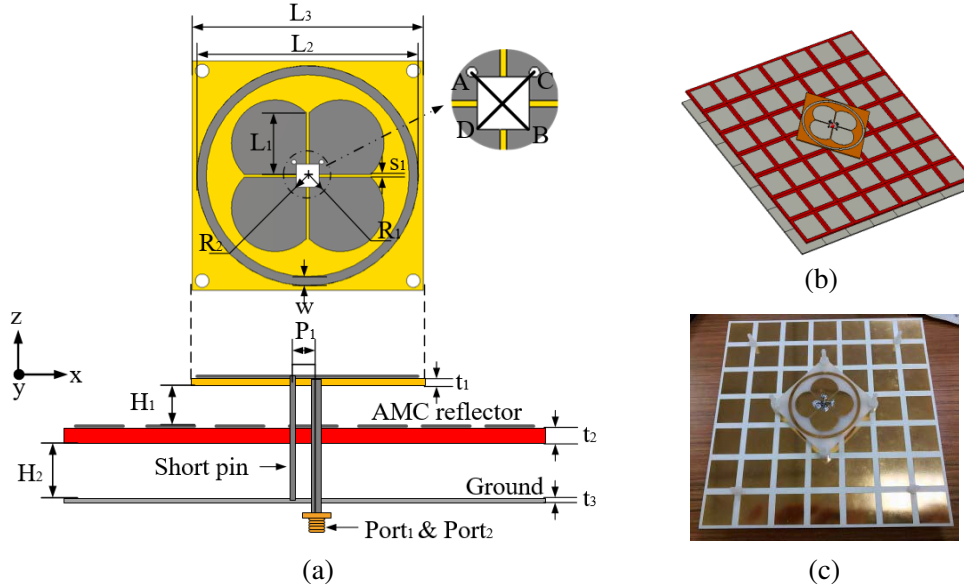


**Figure 1.** The geometry of the proposed antenna (a) with detailed parameters. (b) Overall view. (c) Prototype.

The antenna is fed by two coaxial cables. The outer conductor of one coaxial cable is connected to point B whereas its inner conductor is joined to point A as shown in Fig. 1(a). The same method is used to assemble the other coaxial cable which is connected to point C and D. Two short pins are connected to point A and C separately to improve port isolation.

Detailed parameters of the optimistic antenna are as follows:  $L_1 = 11.6 \text{ mm}$ ,  $L_2 = 48 \text{ mm}$ ,  $L_3 = 50 \text{ mm}$ ,  $R_1 = 19.5 \text{ mm}$ ,  $R_2 = 24 \text{ mm}$ ,  $w = 2 \text{ mm}$ ,  $s_1 = 0.63 \text{ mm}$ ,  $t_1 = 0.8 \text{ mm}$ ,  $t_2 = 1.524 \text{ mm}$ ,  $t_3 = 0.5 \text{ mm}$ ,  $H_1 = 9 \text{ mm}$ ,  $H_2 = 11 \text{ mm}$ .

Current distributions of the proposed antenna at 1.7, 2, and 2.6 GHz for port1 are presented in Fig. 2. As shown in Fig. 2(a), the current mainly flows along the ring at 1.7 GHz, and mainly flows along the dipole which is connected to port1 at 2 GHz and 2.6 GHz as presented in Fig. 2(b) and Fig. 2(c). It can be inferred that the ring introduces the lower resonant frequency, and the dipole introduces the higher resonant frequencies.

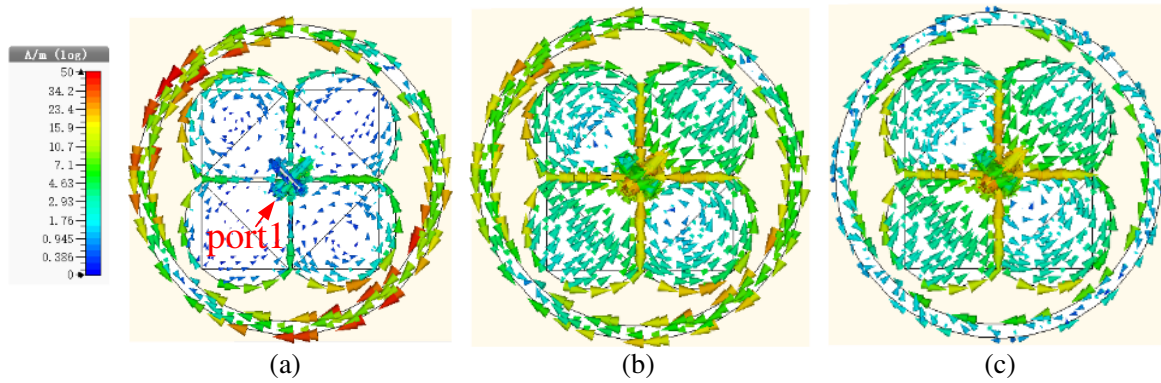


**Figure 2.** Current distribution of the proposed antenna at (a) 1.7 GHz. (b) 2 GHz. (c) 2.6 GHz for port 1.

### 2.2. AMC Reflector

The  $7 \times 7$  AMC array plays an important role in lowering the profile of the proposed antenna, and it is placed under the radiating element as a PEC ground. The geometry of the AMC unit referring to [11] is shown in Fig. 3. The AMC unit is composed of a square patch etched on the substrate of RO4350b ( $\epsilon_r = 3.48$ ,  $\tan \delta = 0.0037$ ) with the thickness of  $t_2$  and a PEC ground as shown in Fig. 3. The distance between them is  $H_2$ .

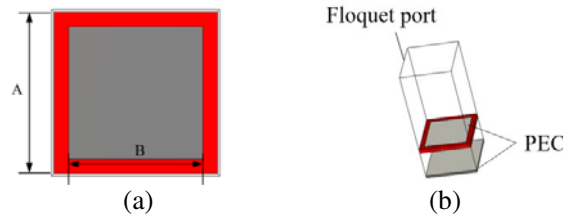


**Figure 3.** (a) The geometry of the AMC unit. (b) Model of AMC unit for analysis.

Computer Simulation Technology (CST) is used to simulate and analyze the performance of this AMC reflector. The simulated reflecting phases of the AMC unit with different lengths of square patch are presented in Fig. 4. With B increasing, the resonant frequency of the AMC reflector will get lower, and the effective phase bandwidth ( $+90^\circ$  to  $-90^\circ$ ) will sharply decrease. To meet the demands of this design, we choose A as 22 mm and B as 18 mm. The effective phase bandwidth of AMC reflector is from 1.65 to 2.9 GHz, which satisfies the 2G/3G/LTE bandwidth.

### 3. RESULTS AND ANALYSIS

To explain the mechanism of the proposed dual-polarized antenna, some key parameters should be carefully discussed. It is noticed through the simulated results that the antenna performance is significantly influenced by the dimension of the ring, short pins, and AMC reflector.

Because of the symmetrical structure of the proposed antenna, there is a small difference between the results of port1 and port2. Thus, only the results of port1 are presented. Fig. 5 gives the  $s$ -parameters of the proposed antenna with and without the ring. As seen in Fig. 5, the ring has a great influence on improving the impedance matching for adding a capacitance between it and dipoles. Thus, the proposed antenna has three resonant frequencies:  $f_1 = 1.67$  GHz,  $f_2 = 2$  GHz, and  $f_3 = 2.66$  GHz. The lowest resonant frequency  $f_1$  is mainly caused by the ring, and  $f_2, f_3$  are produced by the dipole as in [2].

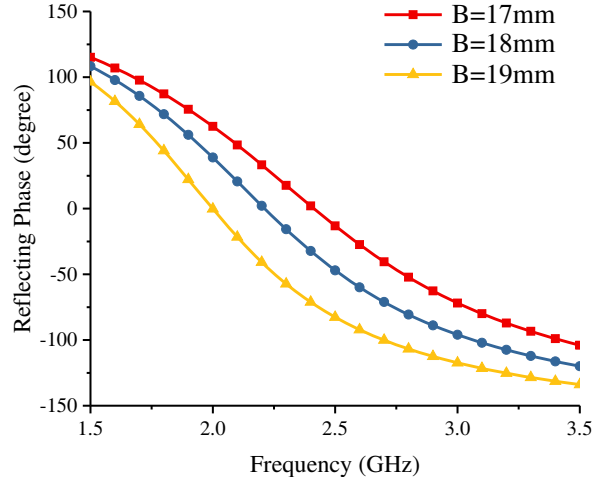


**Figure 4.** The simulated reflecting phases of the AMC unit with different  $B$ .

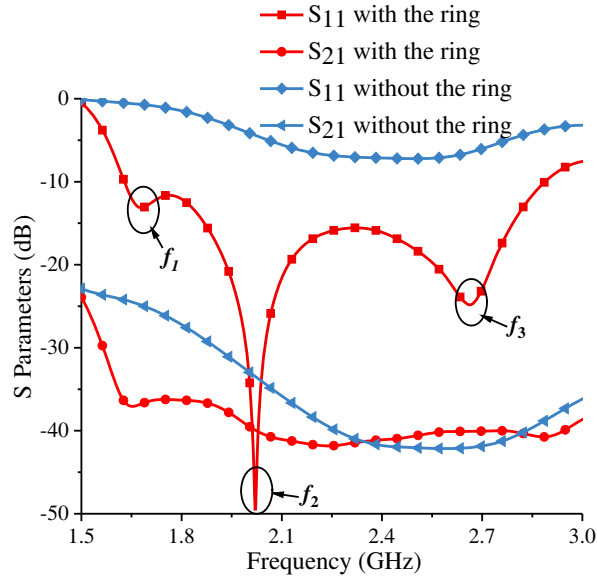
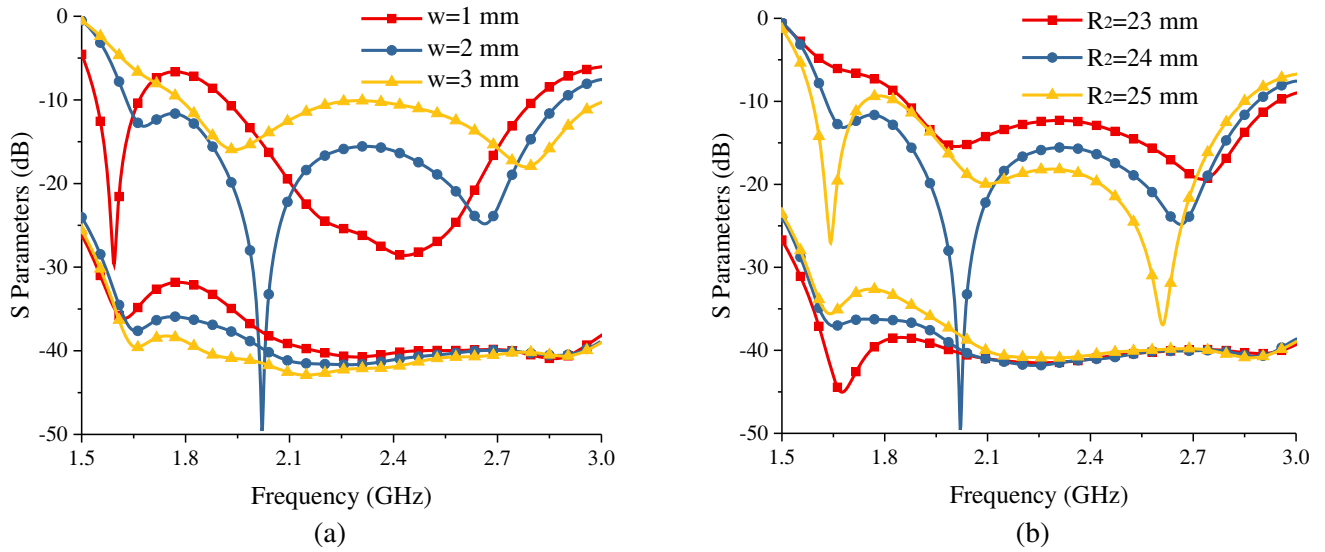


**Figure 5.** The simulated  $s$ -parameters with and without the ring patch.

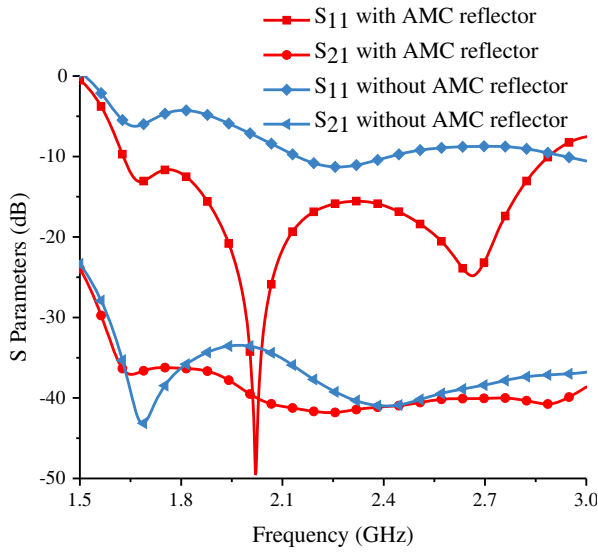
The effects of width and radius of the ring are shown in Fig. 6. As  $w$  increases from 1 mm to 3 mm, the equivalent electrical length of ring patch gets shorter, so  $f_1$  becomes higher. In addition, the port isolation gets better in  $f_1$  and  $f_2$  but has barely changed in  $f_3$ . As  $R_2$  increases, the equivalent electrical length of ring patch gets longer, so  $f_1$  becomes lower. Furthermore,  $S_{21}$  gets worse in  $f_1$  and  $f_2$  but has barely changed in  $f_3$ .

As shown in Fig. 7, the AMC reflector also has an impact on impedance matching and reducing the profile of the proposed antenna. Fig. 8 shows the influence of two short pins on  $s$ -parameters. The outer conductors of the coaxial cables and short pins will produce a balun, which will improve the port isolation. As shown in Fig. 8,  $S_{21}$  without short pins is lower than  $-18$  dB. By introducing two short pins,  $S_{21}$  is lower than  $-33$  dB in the whole bandwidth.

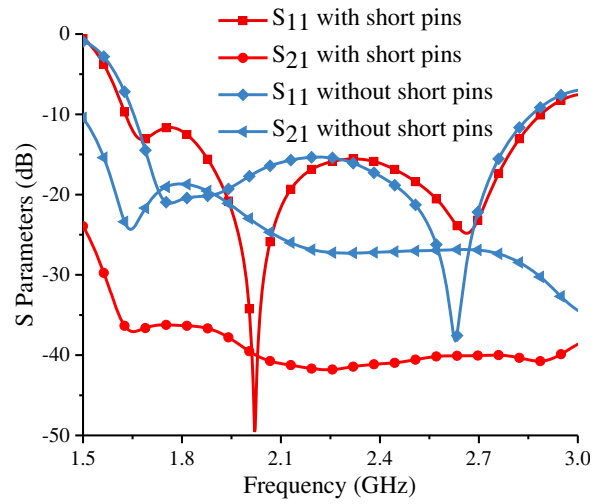
Figure 9 shows the simulated and measured results of  $s$ -parameters. The measured results agree well with the simulated ones. It is seen that the proposed antenna can achieve a wide 10-dB return loss bandwidth of 59% for port1 from 1.6 to 2.94 GHz and 56% for port2 from 1.58 to 2.8 GHz. With short pins, the port isolation is lower than  $-33$  dB in the whole operating band.



**Figure 6.** The simulated *s*-parameters with different (a) *w*. (b) *R*<sub>2</sub>.



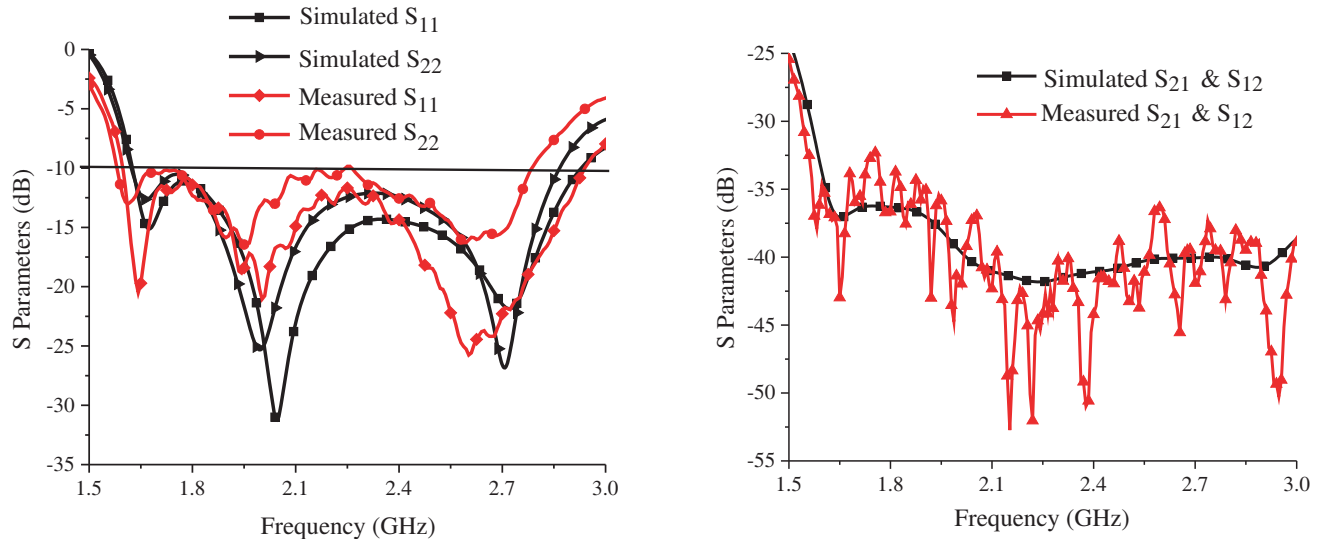
**Figure 7.** The simulated *s*-parameters with and without AMC reflector.



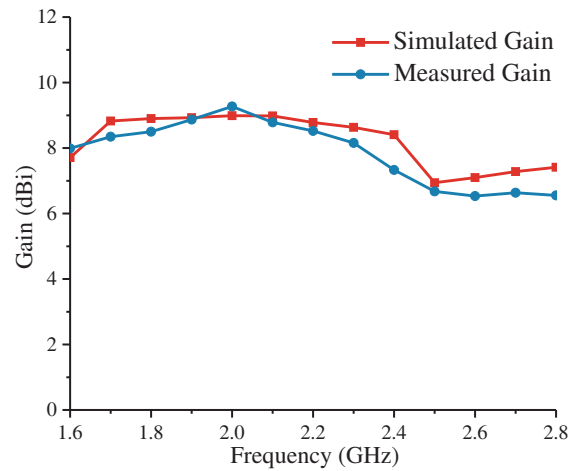
**Figure 8.** The simulated *s*-parameters with and without short pins.

**Table 1.** Comparisons of bandwidth, port isolation, and dimension of compact high-isolation dual-polarized antennas.

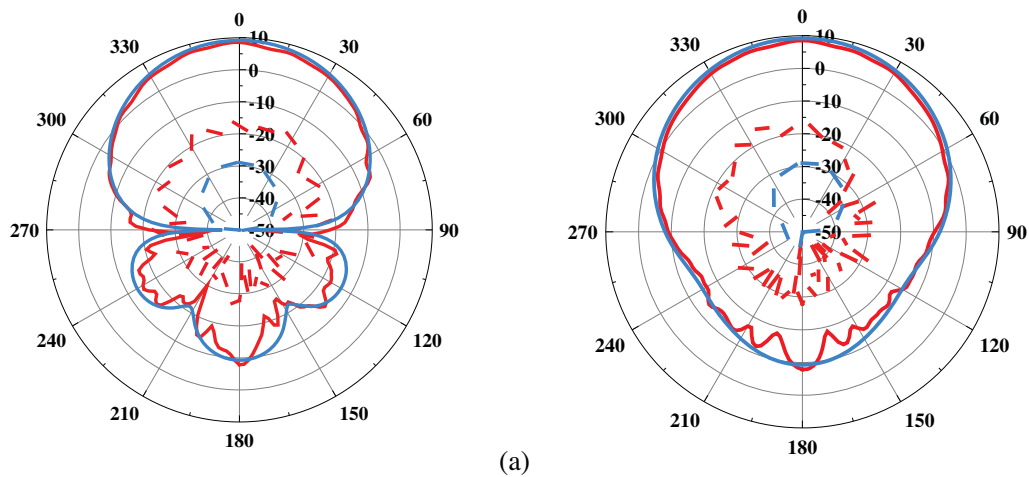
Author	Band Width (GHz)	Port Isolation (dB)	Dimension (mm <sup>3</sup> )
[9]	1.96–2.84	30	43.5 × 43.5 × 16
[10]	2.12–2.77	35	π × 42 <sup>2</sup> × 16.54
[12]	1.64–2.88	25	70 × 70 × 19.6
[13]	1.65–2.81	30	60 × 60 × 18
This Work	1.6–2.78	33	50 × 50 × 22.8



**Figure 9.** The simulated and measured  $s$ -parameters of the proposed antenna.



**Figure 10.** The simulated and measured gain of the proposed antenna.



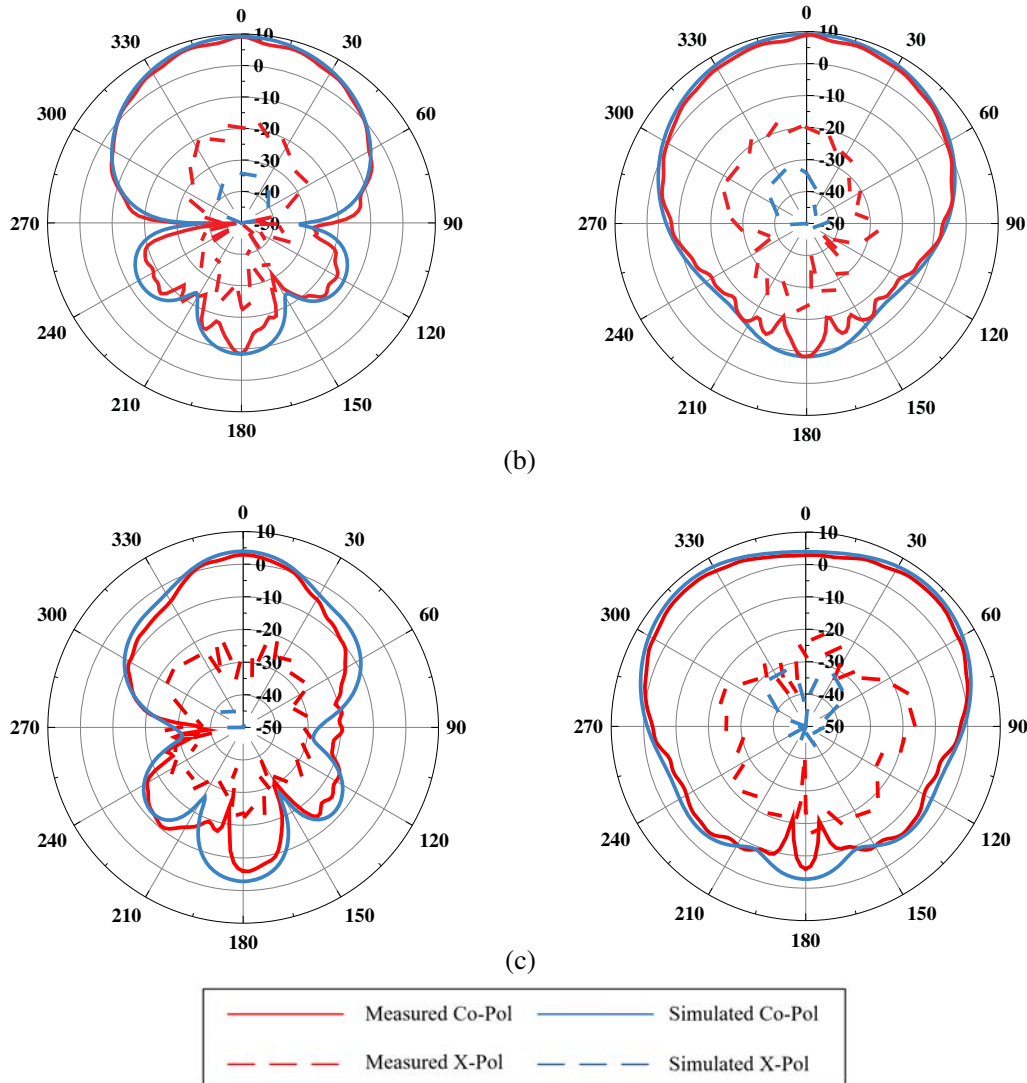


**Figure 11.** The simulated and measured radiation patterns in  $E$ -plane and  $H$ -plane for port1. (a) 1.7 GHz, (b) 2 GHz, (c) 2.6 GHz.

Figure 10 shows the simulated and measured gains of the proposed antenna. The simulated gain of the proposed antenna is around 8 dBi. The measured gain is lower than the simulated results due to the fabrication error and measuring error. The simulated and measured radiation patterns of  $E$ -plane and  $H$ -plane at the frequencies of 1.7, 2.0, and 2.6 GHz of port1 are depicted in Fig. 11. The cross-polarization is about 30 dB.

Bandwidths for  $S_{11} < -10$  dB of compact dual-polarized base station antennas are summarized in Table 1 together with port isolations and dimensions of the antennas. The antenna in this paper has properties as wide bandwidth, high port isolation and compact dimension.

#### 4. CONCLUSION

A compact high-isolation dual-polarized antenna is presented in this paper. Two orthogonal bow-tie patches with a circular ring around them are adopted to widen its impedance bandwidth from 1.6 GHz to 2.78 GHz for both ports. Two short pins are added to improve the port isolation of the proposed antenna. Furthermore, a  $7 \times 7$  AMC array is introduced to lower the profile of the antenna to only  $0.16\lambda_0$ . The gain of the proposed antenna is about 8 dBi, and the cross-polarization is about 30 dB.

Thanks to these properties, the proposed antenna is a strong contender for 2G/3G/LTE base station and WLAN/WiMAX applications.

## ACKNOWLEDGMENT

This work was supported by the National Natural Science Foundation of China (No. 61701041 and No. 61327806).

## REFERENCES

1. Wang, B., C. Huang, H. Hao, B. Yin, and W. Luo, "Broadband dual-polarized dipole antenna with metallic cylinder for base station," *Electromagnetics*, Vol. 36, 515–523, 2016.
2. Cui, Y. H., R. L. Li, and H. Z. Fu, "broadband dual-polarized planar antenan for 2G/3G/LTE base stations," *IEEE Transaction on Antennas and Propagation*, Vol. 62, 4836–4840, 2014.
3. Yang, Z., C. Zhang, Y. Z. Yin, and Y. Wang, "A wideband dual-polarized modified bowtie antenna for 2g/3g/lte base-station applications," *Progress In Electromagnetics Research Letters*, Vol. 61, 131–137, 2016.
4. Lian, R. N., Z. D. Wang, Y. Z. Yin, J. J. Wu, and X. Y. Song, "Design of a low-profile dual-polarized stepped slot antenna array for base station," *IEEE Antennas and Wireless Propagation Letters*, Vol. 15, 362–365, 2016.
5. Li, B., Y. X. Z. Yin, W. Hu, Y. Ding, and Y. Zhao, "Wideband dual-polarized patch antenna with low cross polarization and high isolation," *IEEE Antennas Wireless Propag. Letters*, Vol. 11, No. 4, 427–430, 2012.
6. Li, L., B. Feng, and M. Wang, "A low-profile dual-polarized magneto-electric dipole antenna with metamaterial loading and anti-interference capability," *IEEE International Symposium on Electromagnetic Compatibility*, 1–3, 2017.
7. Kaddour, A. S., "Low profile dual-polarized wideband antenna," *International Symposium on Antennas and Propagation*, Okinawa, Japan, 2017.
8. Li, Z., Y. Sun, M. Yang, Z. Wu, and P. Tang, "A broadband dual-polarized magneto-electric dipole antenna for 2G/3G/LTE/WiMAX applications," *Progress In Electromagnetics Research C*, Vol. 73, 127–136, 2017.
9. Hu, W., R. N. Lian, Z. Y. Tang, and Y. Z. Yin, "Wideband, low-profile, dual-polarized slot antenna with an AMC surface for wireless communications," *International Journal of Antenna and Propagation*, Vol. 2016, 1–8, 2016.
10. Ren, J., B. Wang, and Y. Z. Yin, "Low profile dual-polarized circular patch antenna with an AMC reflector," *Progress In Electromagnetics Research Letters*, Vol. 47, 131–137, 2014.
11. Wu, J., "A low profile dual-polarized wideband omnidirectional antenna based on AMC reflector," *IEEE Transactions on Antennas and Propagation*, Vol. 65, 368–374, 2017.
12. Li, M., Q. L. Li, B. Wang, C. F. Zhou, and S. W. Cheung, "A low-profile dual-polarized dipole antenna using wideband AMC reflector," *IEEE Transactions on Antennas and Propagation*, Vol. 66, 2610–2615, 2018.
13. Wang, B., "Low-profile broadband dual-polarized dipole antenna on AMC reflector for base station," *Progress In Electromagnetics Research C*, Vol. 74, 171–179, 2017.
14. Lin, J., "A low-profile dual-band dual-mode and dual-polarized antenna based on AMC," *IEEE Antennas and Wireless Propagation Letters*, Vol. 16, 2473–2476, 2017.